COMBINATION OF MLS, GA & CG FOR THE REDUCTION OF RCS OF MULTILAYERED CYLINDRICAL STRUCTURES COMPOSED OF DISPERSIVE METAMATERIALS

H. Oraizi and A. Abdolali

Department of Electrical Engineering
Iran University of Science and Technology
Narmak, Tehran 1684613114, Iran

Abstract—In this paper the electromagnetic wave scattering from multilayered cylindrical structures is studied for a normally incident plane wave with linear (TE or TM), circular and elliptical polarizations. The cylindrical layers may be composed of any combination of dispersive common materials and metamaterials. The addition theorems for the cylindrical waves are used for the EM wave analysis. The objective of this study is to decrease or increase the Radar Cross Section (RCS) in an ultra wide band width. The optimization is based on the Method of Least Squares (MLS), employing a novel combination of the Genetic Algorithm (GA) and Conjugate Gradient (CG), where the global search for the minimization point is performed by GA and the local search is done by CG, which greatly speeds up the search algorithm. The behaviors of various combinations of common materials and metamaterials for reduction of RCS are studied. Furthermore, the procedures for selection of correct signs for metamaterial parameters, namely ε, μ, k and η are presented.

1. INTRODUCTION

Minimization or even maximization of radar cross section (RCS) [1–3] of objects is of particular interest, which can be achieved by different techniques such as application of Radar Absorbing Materials (RAM) [4, 6]. Other applications of RAM have been developed, such as anechoic chambers, antenna designs with low side lobes, protection from electromagnetic interference in high speed circuits, etc. Achievement of a wide frequency band performance requires correct geometrical formations and application of appropriate RAM. In this regard planar structures have been mostly studied. However,

in this paper we investigate multilayered cylindrical structures, which may be considered as basic and canonical shapes of practical objects. We use the combination of common materials and metamaterials designated as Double Positive (DPS), Double Negative (DNG), ε Negative (ENG) [7], and μ Negative (MNG) [8] as RAM for the reduction of RCS. In many studies the quasi-static values of ε and μ are used [9], which are constants at all frequencies. However, here we use their various dispersive relations, which lead to accurate results in the entire frequency spectrum. The frequency spectrum for RCS is divided into three regions [3]: (1) Low frequency or Rayleigh region; (2) High frequency region (or visible light); (3) The middle frequency region or resonance region, where the object dimensions are comparable with the wavelengths and the common low frequency and high frequency approximations are not applicable. Computation of radar cross-section in the middle frequency range requires the application of full-wave numerical techniques, such as MOM, FDTD, TLM, FEM, etc [8, 9]. Several studies have been performed for the analysis of electromagnetic and optical scattering of layered cylinders composed of isotropic and anisotropic materials and also arrays of such structures in various configurations [10–14].

Metamaterials (MTMs) were first postulated and theoretically studied by Veselago [15] in 1969. Various applications for MTMs — specially in plannar structure — has been done [16–18]. However, here we are concerned with the macroscopic properties of metamaterials, where the values of permittivity and permeability are described by the appropriate Drude, Lorentz and resonance models.

In general, electromagnetic wave scattering from multilayered cylindrical structures is studied by analytical, approximate and numerical methods. Here we use the theoretical method of addition theorem, where the fields are expanded in terms of the cylindrical eigen functions in various media [3].

The TE, TM and circular polarizations are considered for the normally incident wave. The multilayered cylindrical structure may have any number of layers composed of any type of common materials and/or metamaterials. The core cylinder may be made up of PEC, dielectric material or metamaterial. The frequency spectrum is arbitrary. Both the monostatic and bistatic radars may be treated. The method of least squares [19] is used for the optimization of RCS. The numerical algorithm is written in a general way to treat all the above mentioned cases. The selection of correct signs for the real and imaginary parts of intrinsic impedance (η) and wave number (k) of metamaterials are considered in some detail, in order to avoid any errors in computations.

2. COMMON MATERIALS AND METAMATERIALS FOR RAM

Various combinations of lossy and lossless materials and metamaterials are used in this paper for RAM such DPS ($\text{Re}(\varepsilon) > 0$, $\text{Re}(\mu) > 0$), DNG ($\text{Re}(\varepsilon) < 0$, $\text{Re}(\mu) < 0$), ENG ($\text{Re}(\varepsilon) < 0$, $\text{Re}(\mu) > 0$), and MNG ($\text{Re}(\varepsilon) > 0$, $\text{Re}(\mu) < 0$). Here we use the dispersion relations of ε and μ for common materials (designated as right-handed, RH), which are summarized in Table 1.

Table 1. List of right-handed materials used for coating layers. The materials listed are generic right-handed lossy materials taken from [20]. Frequencies are listed in GHz.

Class of materials	Permittivity model	Permeability model	Parameters Ranges
Lossless dielectric	$\varepsilon = \varepsilon_r$	$\mu = 1$	$1 \leq \varepsilon_r \leq 25$
Lossless magnetic	$\varepsilon = \varepsilon_r$	$\mu = \mu_r$	$1 \leq \varepsilon_r \leq 25$ $1 \leq \mu_r \leq 25$
Lossy dielectric	$\varepsilon = \frac{\varepsilon_r}{f^\alpha} + j\frac{\varepsilon_i}{f^\beta}$	$\mu = \mu_r$	$1 \leq \varepsilon_r, \varepsilon_i, \mu_r \leq 25$ $0 \leq \alpha, \beta \leq 1$
Lossy magnetic	$\varepsilon = \varepsilon_r$	$\mu = \frac{\mu_r}{f^\alpha} + j\frac{\mu_i}{f^\beta}$	$1 \leq \varepsilon_r, \mu_r, \mu_i < 25$ $0 \leq \alpha, \beta \leq 1$
Relaxation-type magnetic	$\varepsilon = \varepsilon_r$	$\mu = \frac{\mu_m(f_m^2 + jf_m f)}{f^2 + f_m^2}$	$1 \leq \varepsilon_r \leq 25$ $1 \leq \mu_m \leq 25$ $1 \leq f_m \leq 30$

The real and imaginary parts of permeability for lossy magnetic and relaxation-type magnetic materials are drawn in Fig. 1. Those of permittivity for lossy dielectric materials are similar to lossy magnetic materials as shown in Fig. 1.

The dispersion relations of metamaterials (designated as left-handed, LH) are summarized in Table 2. The negative real part of permittivity may be realized by an array of rods and that of permeability by an array of split ring resonators (SRR).

The real and imaginary parts of ε and μ for rings and rods embedded in materials are drawn versus frequency in the range 5–20 GHz in Fig. 2 using the dispersion relations in Table 2.

It is observed that all the four classes of materials are realizable by the rings and rods embedded media. The range of frequencies, where the behaviors due to DNG, ENG and MNG media are observed,
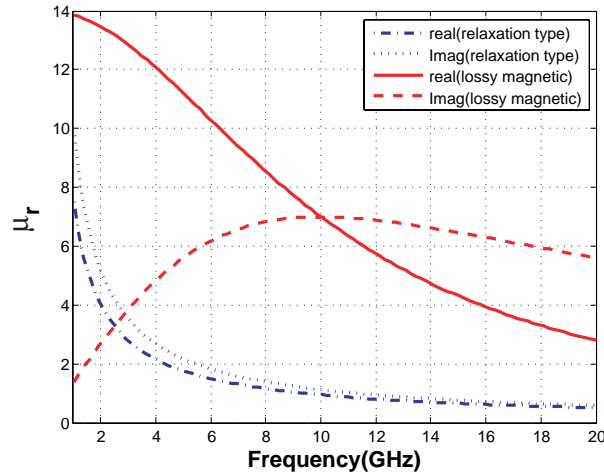
Figure 1. Examples of the permeability of two classes of right-handed materials used in the design of RAMs. Lossy magnetic: $\mu_r = 7.5$, $\mu_i = 10$, $\alpha = 0.9$, $\beta = 0.95$; Relaxation-type: $f_m = 10\,\text{GHz}$, $\mu_m = 14$.

Table 2. List of LH metamaterials used for coating layers. The three classes of materials shown are based on conventional models for LH metamaterials composed of metallic rods and rings. Frequencies are listed in GHz [21].

Class of materials	Permittivity model	Permeability model	Parameters ranges
ENG (Rods only)	$\varepsilon = 1 - \dfrac{f_{ep}^2}{f^2 + jf\gamma_e}$	$\mu = 1$	$1 \leq f_{ep} \leq 30$ $0.001 \leq \gamma_e \leq 5$
MNG (Rings only)	$\varepsilon = 1$	$\mu = 1 - \dfrac{f_{mp}^2 - f_{mo}^2}{f^2 - f_{mo}^2 + jf\gamma_m}$	$1 \leq f_{mo} \leq 30$ $f_{mp} \sim f_{mo} + [0.1, 5]$ $0.001 \leq \gamma_m \leq 5$
DNG (Rods & Rings)	$\varepsilon = 1 - \dfrac{f_{ep}^2}{f^2 + jf\gamma_e}$	$\mu = 1 - \dfrac{f_{mp}^2 - f_{mo}^2}{f^2 - f_{mo}^2 + jf\gamma_m}$	Same as above

are depicted in Fig. 2. Consequently, the dispersion relations of DNG or LH medium behave differently in various parts of the frequency spectrum depending on the values of their parameters. On the other hand, the dispersion relations of DPS or RH materials behave
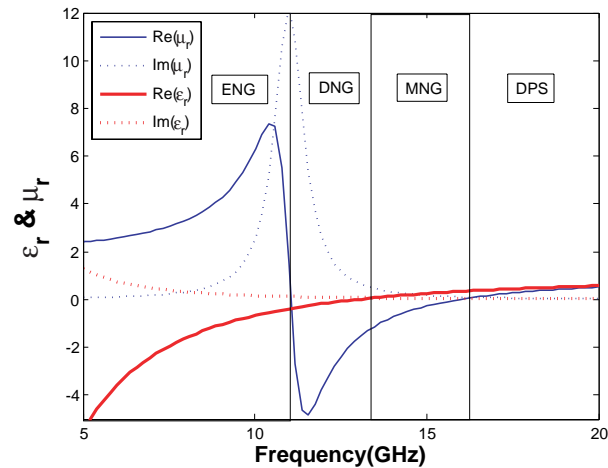
Figure 2. Real & imaginary parts of permittivity & permeability of Rods & Rings media versus frequency for the following parameters: $\gamma_m = 1\,\mathrm{GHz}$, $f_{mp} = 16\,\mathrm{GHz}$, $f_{mo} = 11\,\mathrm{GHz}$, $\gamma_e = 1\,\mathrm{GHz}$, $f_{ep} = 13\,\mathrm{GHz}$.

identically across the frequency spectrum.

The optimization of RCS by the method of least squares using a minimization algorithm such as the Genetic Algorithms [22], is performed on the layer thicknesses and all the parameters in the dispersion relations given in Tables 1 and 2. The optimization process may be somewhat time consuming due to the large number of parameters.

3. ANALYTICAL DEVELOPMENT

Consider a cylindrical core of radius 'a' covered by several coaxial layers of radii 'b', 'c', ... made of common materials or metamaterials. The core cylinder may be made of PEC (such as supporting columns on shipboards) or dielectric materials (such as fiberglass columns) as shown in Fig. 3.

Consider a plane wave normally incident on a multilayered cylindrical structure as shown in Fig. 3. The time dependence is chosen as $e^{-j\omega t}$. The incident plane wave may be TE (with $E_z = 0$), TM ($H_z = 0$) or circularly polarized ($E_z \neq 0$ and $H_z \neq 0$). We consider the TM electromagnetic fields and expand the incident and scattered fields from the cylindrical structure and also the standing waves inside the layered media and the cylindrical core by the application of addition
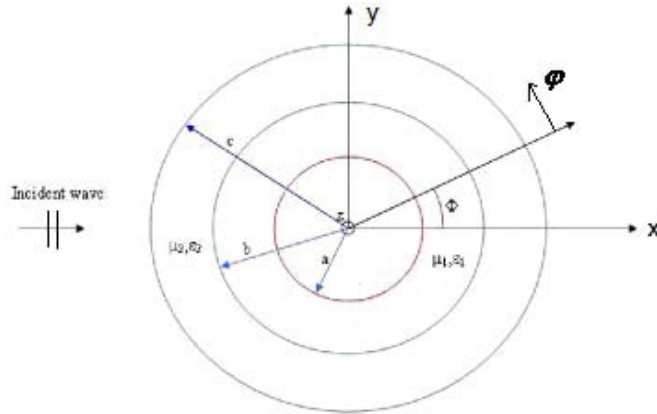
Figure 3. Geometrical configuration of the multilayered cylindrical structure.

theorem [3]:

$$
\text{Incident Wave}:
\begin{cases}
E_{zi} = \displaystyle\sum_{n=-\infty}^{+\infty} j^n J_n(k_0 r) e^{jn(\varphi-\varphi_0)} \\
H_{\varphi i} = \dfrac{j}{\eta_0} \displaystyle\sum_{n=-\infty}^{+\infty} j^n J_n'(k_0 r) e^{jn(\varphi-\varphi_0)}
\end{cases}
\tag{1}
$$

$$
\text{Scattered Wave}:
\begin{cases}
E_{zs} = \displaystyle\sum_{n=-\infty}^{+\infty} A_{ns} J^n H_n^{(1)}(k_0 r) e^{jn(\varphi-\varphi_0)} \\
H_{\varphi s} = \dfrac{j}{\eta_0} \displaystyle\sum_{n=-\infty}^{+\infty} A_{ns} J^n H_n'^{(1)}(k_0 r) e^{jn(\varphi-\varphi_0)}
\end{cases}
\tag{2}
$$

l'th Layer Wave:

$$
\begin{cases}
E_{zl} = \displaystyle\sum_{n=-\infty}^{+\infty} [C_{nl} J_n(k_l r) + D_{nl} Y_n(k_l r)] e^{jn(\varphi-\varphi_0)} \\
H_{\varphi l} = \dfrac{j}{\eta_l} \displaystyle\sum_{n=-\infty}^{+\infty} [C_{nl} J_n'(k_l r) + D_{nl} Y_n'(k_l r)] e^{jn(\varphi-\varphi_0)}
\end{cases}
\tag{3}
$$

and if the cylindrical core is a dielectric material or a metamaterial,

then the core's interior fields can be expressed as:

$$\text{Core's Interior Wave} : \begin{cases} E_{zc} = \displaystyle\sum_{n=-\infty}^{+\infty} P_{nc} J_n(k_c r) e^{jn(\varphi-\varphi_0)} \\ H_{\varphi c} = \dfrac{j}{\eta_c} \displaystyle\sum_{n=-\infty}^{+\infty} P_{nc} J_n'(k_c r) e^{jn(\varphi-\varphi_0)} \end{cases} \quad (4)$$

where J_n and Y_n are the Bessel functions of the first and second kinds of degree n, respectively, and H_n is the Hankle function of first kind and degree n. Notation($'$) refers to the derivative with respect to the argument. Wave number k_l and intrinsic impedance η_l refer to the l'th layer:

$$k_l = \omega\sqrt{\mu_l \varepsilon_l}$$
$$\eta_l = \sqrt{\frac{\mu_l}{\varepsilon_l}} \quad (5)$$

where k_0 and η_0 refer to those of the free space outside the cylindrical structure. Amplitudes A_{ns}, C_{nl}, D_{nl} and P_{nc} are unknown, which are determined by enforcing the boundary conditions namely continuity of tangential E and H fields at the cylindrical boundaries and also vanishing of tangential electric fields on PEC. This leads to a linear matrix equation in terms of unknown amplitudes. The TE fields are dual of the TM fields. It should be noted that the normal incidence of TE or TM fields on a multilayered cylindrical structure does not create any mutual coupling, and as a result may be analyzed separately.

Now, RCS in two dimensional systems is defined as [1]:

$$\sigma = \lim 2\pi r \left|\frac{E_s}{E_i}\right|^2 \qquad r \to \infty \quad (6)$$

By using the asymptotic formulas for Hankle functions as the distance 'r' approaches infinity, the normalized bistatic RCS may be simplified as:

$$\text{TM} : \frac{\sigma}{\lambda} = \frac{2}{\pi} \left| \sum_{n=-\infty}^{+\infty} A_{ns} e^{jn(\varphi-\varphi_o)} \right|^2$$

$$\text{TE} : \frac{\sigma}{\lambda} = \frac{2}{\pi} \left| \sum_{n=-\infty}^{+\infty} B_{ns} e^{jn(\varphi-\varphi_o)} \right|^2 \quad (7)$$

where φ_0 is the direction of incident wave and φ is the direction of scattered field. And A_{ns} & B_{ns} are the amplitudes of scattered waves

for TM & TE polarization, respectively. The monostatic RCS may be obtained by $\varphi_0 = 0$ and $\varphi = \pi$. For the case of circularly polarized plane wave, the electric field is:

$$\bar{E}_{ti} = (E_{\varphi i}\hat{\varphi} \pm jE_{zi}\hat{z}) = E_0 e^{-jk_0 r}(\hat{\varphi} \pm j\hat{z}) \tag{8}$$

where signs $+$ and $-$ indicate right-handed and left-handed waves, respectively. The circularly and elliptically polarized waves are some combinations of TE and TM waves. Consequently, the reflected wave is elliptically polarized:

$$\bar{E}_{ts} = (E_{\varphi s}\hat{\varphi} \mp E_{zs}\hat{z}) \tag{9}$$

Therefore, the normalized RCS for circularly polarized wave may be obtained as

$$|E_{ts}|^2 = |E_{\varphi s}|^2 + |E_{zs}|^2$$

$$|E_{ti}|^2 = |E_{\varphi i}|^2 + |E_{zi}|^2 = 2E_0^2 \tag{10}$$

$$\sigma = \lim 2\pi r \left|\frac{E_{ts}}{E_{ti}}\right|^2 \qquad r \to \infty \tag{11}$$

4. SELECTION OF CORRECT SIGNS FOR THE REAL AND IMAGINARY PARTS OF ε, μ, K AND η

Veselago [15] indicated that for DNG media, the following formula may be used for the wave number:

$$k = \omega\sqrt{\mu\varepsilon} = \omega\sqrt{(-|\mu|)(-|\varepsilon|)} = \omega\sqrt{e^{j\pi}|\mu|\, e^{j\pi}|\varepsilon|} = -\omega\sqrt{\mu\varepsilon} \tag{12}$$

However, the correct sign for the real and imaginary parts of the wave number k and intrinsic impedance of metamaterials DNG, ENG, and MNG should be selected by using appropriate formulas.

For all types of metamatarials, the permittivity and permeability may be taken as $\varepsilon = \pm\varepsilon' \pm j\varepsilon''$ and $\mu = \pm\mu' \pm j\mu''$, which lead to 16 different cases. However, according to the Poynting's theorem, for time dependence as $e^{+j\omega t}$, the imaginary parts of ε and μ should be negative and for $e^{-j\omega t}$, they should be positive, namely $\text{Im}(\varepsilon) \geq 0$ and $\text{Im}(\mu) \geq 0$. For our case $e^{-j\omega t}$, the conditions $\varepsilon = \pm\varepsilon' + j\varepsilon''$ and $\mu = \pm\mu' + j\mu''$ lead to four cases denoted by DPS, DNG, ENG and MNG. The apparent difference among dispersion relations in various references is due to the assumption of time dependence as $e^{\pm j\omega t}$.

Now, we write the wave number as:

$$k = \omega\sqrt{\mu\varepsilon} = \text{Re}(k) + j\text{Im}(k) \tag{13}$$

and the wave traveling in the positive $+r$ direction as:

$$e^{\pm jkr} = e^{\mp r\text{Im}(k)} e^{\pm jr\text{Re}(k)} \tag{14}$$

corresponding to the selection of time dependences as $e^{\mp j\omega t}$ respectively, which lead to $\text{Im}(k) > 0$ and $\text{Im}(k) < 0$, respectively so that the traveling wave would attenuate in the positive $+r$ direction. In case the medium is lossless, $\text{Im}(k) = 0$.

The intrinsic impedance of a medium may be written as:

$$\eta = \sqrt{\frac{\mu}{\varepsilon}} = \text{Re}(\eta) + j\text{Im}(\eta) \tag{15}$$

Therefore, in order for the medium to be passive, the real part of η should be positive, namely $\text{Re}(\eta) > 0$, otherwise the medium would be active, which is unphysical. The same conclusion would be arrived at by considering the equivalent transmission line of the medium.

For the time dependence $e^{-j\omega t}$, the characteristic parameters of metamaterials may be written as:

$$\varepsilon = \pm\varepsilon' + j\varepsilon'' = |\varepsilon| \angle \theta_\varepsilon$$

$$\mu = \pm\mu' + j\mu'' = |\mu| \angle \theta_\mu$$

$$k = \pm k' + jk'' = |k| \angle \theta_k \tag{16}$$

$$\eta = \eta' \pm j\eta'' = |\eta| \angle \theta_\eta$$

where the values of ε', ε'', μ', μ'', k', k'', η' and η'' are assumed positive. The conditions for the lossy media are $\text{Im}(\varepsilon) \geq 0$, $\text{Im}(\mu) > 0$, $\text{Im}(k) > 0$ and $\text{Re}(\eta) > 0$. Since the square root may have positive or negative sign for DPS, DNG, ENG and MNG media, the phases θ_ε, θ_μ, θ_k and θ_η are as indicated in Table 3. It should be noted that we have two choices; the first choice and the second choice. The second choice is obtained by increasing the phase by π. For the lossless case, the computation by Eqs. (13) and (15) should be corrected. For example, for lossless DNG, formula (13) gives $k = +k'$, whereas $k = -k'$ is correct.

For the lossless ENG, formula (15) gives $\eta = +j\eta''$, whereas $\eta = -j\eta''$ is correct, as shown in Table 3.

Table 3. The range of variations of ε, μ, k and η and selection of correct signs for their real and imaginary parts. The lossy and lossless cases are given for DNG, ENG and MNG (RPV: Range of Phase Variation, SRP: Sign of Real Part, SIP: Sign of Imaginary Part).

DNG	ε	μ	k	η
RPV	$(\frac{\pi}{2}, \pi)$	$(\frac{\pi}{2}, \pi)$	$(\frac{\pi}{2}, \pi)$	$(0, \frac{\pi}{2})$
SRP	$-$	$-$	$-$	$+$
SIP	$+$	$+$	$+$	$-, +$
Lossless DNG	$\varepsilon = -\varepsilon'$	$\mu = -\mu'$	$k = -k'$	$\eta = +\eta'$
ENG	ε	μ	k	η
RPV	$(\frac{\pi}{2}, \pi)$	$(0, \frac{\pi}{2})$	$(\frac{\pi}{4}, 3\frac{\pi}{4})$	$(-\frac{\pi}{2}, 0)$
SRP	$-$	$+$	$+, -$	$+$
SIP	$+$	$+$	$+$	$-$
Lossless ENG	$\varepsilon = -\varepsilon'$	$\mu = +\mu'$	$k = +jk''$	$\eta = -j\eta''$
MNG	ε	μ	k	η
RPV	$(0, \frac{\pi}{2})$	$(\frac{\pi}{2}, \pi)$	$(\frac{\pi}{4}, 3\frac{\pi}{4})$	$(0, \frac{\pi}{2})$
SRP	$+$	$-$	$+, -$	$+$
SIP	$+$	$+$	$+$	$+$
Lossless MNG	$\varepsilon = +\varepsilon'$	$\mu = -\mu'$	$k = +jk''$	$\eta = +j\eta''$

5. OPTIMIZATION OF RCS BY MLS USING THE COMBINATION OF GA AND CG

We intend to optimize the RCS in a frequency band by minimizing the following least square error function [19]:

$$error\ function = \sum_{i=1}^{n_f} W_i (\text{RCS}_i - C_i)^2 \qquad (17)$$

where the desired frequency band is divided into n_f discrete frequencies f_i at which RCS_i is to have the specified value C_i and W_i is a weighting function at f_i. The error function is a complicated function of the structure geometry (radius of core cylinder, number of cylindrical layers and their thicknesses), various parameters in the dispersion relations of permittivity and permeability, incidence angle of plane waves, polarization (TE, TM, circular, elliptical), etc. Consequently, the optimization of error function is quite difficult due to its complex nature and large number of variables.

For example, consider the RCS of a long conducting cylinder of

radius $a = 50\,$mm covered by a dielectric layer of thickness $b - a = 50\,$mm and material constants ε_r and μ_r. The RCS is drawn in 3-D in Fig. 23 in [9] as a function of ε_r and μ_r for their values of 0.05 to 30 at frequency $f = 5\,$GHz and normal incidence of a TE plane wave. It is seen that there are many extrema in this complex figure, which make the process of optimization very difficult.

Therefore, we propose to use a combination of Genetic Algorithm (GA) [23] and Conjugate Gradient Method (CG) [24] for the minimization of error function. Since GA as an evolutionary algorithm is supposed to be a global optimization method, it does not heavily depend on the initial values of the variables. However, implementation of GA is very computer time consuming. On the other hand, CG is largely a local optimization method and its convergence to an extremum point depends on the initial values of variables. However, implementation of CG is relatively fast, but it requires the computation of gradients of functions. Consequently, combination of GA and CG may utilize the advantages of each one, avoiding the shortcomings of both. Therefore, the combined algorithm starts by implementing GA with a set of initial values for variables which leads towards an extremum. At about this point, GA is stopped and CG is activated to speed up the convergence towards a local extremum. Thereafter, the values of variables at this extremum point are taken as the initial values for GA. This algorithm is continued until the global extremum is arrived at.

6. NUMERICAL EXAMPLES

Several examples of minimization of RCS are provided below.

Example 1. Consider a conducting cylinder of radius $a = 4.71\,$mm covered by a dielectric layer with material constants $\varepsilon_r = 2.54$ and $\mu_r = 1$ and thickness '$b - a$'. The operating frequency is $f = 9.57\,$GHz, the wave number in free space is $k_0 = 200$ and the wave number in the dielectric layer is $k_1 = 318.7$. The polarization of incident wave is TM. The normalized RCS is computed by the proposed method and drawn versus $k_1 b$ in Fig. 3 in [9], and is compared with the experimental results of the same problem in reference [25]. The two data are in perfect agreement.

In the following examples, the frequency band-width is taken as 1–10 GHz the number of discrete frequencies is $n_f = 50$, the variables of optimization are the thicknesses of layers and the parameters in the dispersion relation of metamaterials.

Example 2. Consider a conducting cylinder of radius $a = 50\,$mm covered by two layers composed of nondispersive metamaterials

with normally incident TE plane wave. The permittivity and permeability of metamaterials are assumed independent of frequency, which is unphysical. The optimization of RCS is performed for the aforementioned four types of metamaterials. The signs of ε, μ, k and η should be selected according to Table 3. Since no signal dissipation occurs inside the layer materials, the RCS reduction is solely due to the diversion of incident plane wave towards directions other than that of radar transmitter. The optimum values of layer thicknesses, permittivity and permeability are given in Table 4.

Table 4. Thickness,permittivity & permeability of a coating materials obtained after minimization of RCS of a conducting cylinder ($a = 50\,$mm) in the frequency band $[1$–$10]\,$GHz for TE polarization with two layers of coating made of nondispersive materials.

Class of materials	Thickness of layer (mm)	ε_r	μ_r
First layer: DNG	3.5874	−24.7180	−2.4259
Second layer: DNG	7.5273	−0.0171	−3.6853
First layer: DPS	8.5235	0.0327	0.01
Second layer: DNG	1.6542	−2.4176	−2.2551
First layer: DPS	11.2	0.0414	0.1296
Second layer: DPS	0.4	3.5764	1.3639
First layer: ENG	15.0876	−8.0948	1.3493
Second layer: MNG	3.3590	0.0103	−0.2697

The optimum RCS's for different metamaterials are drawn versus frequency and are compared with that due to a bare PEC cylinder in Fig. 4.

It is observed that the combination of DNG-DNG does not result in an appreciable reduction of RCS. However, other combinations provide good RCS reduction in different frequency bands. For example, ENG-MNG provides good RCS reduction in the 2–5 GHz band width. Consequently, if RCS reduction is required in a particular frequency band, optimization of RCS should be tried by different combinations of metamaterial coatings.

Example 3. The parameters of this example are the same as those of example 2, except that the incident plane wave is TM. The results of RCS optimization are given in Table 5 and drawn in Fig. 5 versus frequency.

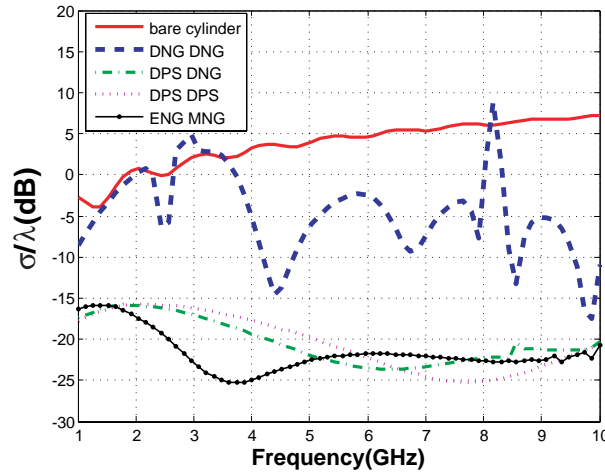It is seen that the best case is the combination DPS-DPS.

Figure 4. A comparison of normalized RCS of a conducting cylinder ($a = 50$ mm) for TE polarization without coating and with two layer coating of nondispersive materials.

Table 5. Thickness,permittivity & permeability of two coating layers made of nondispersive materials on a conducting cylinder ($a = 50$ mm) after minimization of RCS in the frequency band [1–10] GHz for TM polarization.

Class of materials	Thickness of layer (mm)	ε_r	μ_r
First layer: DNG	18.9686	−0.2532	−12.4858
Second layer: DNG	1.3433	−5.1192	−2.8222
First layer: DPS	17.0308	5.5212	0.1135
Second layer: DNG	1.9582	−6.2342	−2.1868
First layer: DPS	22.02	0.014	26.38
Second layer: DPS	5.8	0.0575	0.0155
First layer: ENG	0.3868	−2.5396	3.5767
Second layer: MNG	1.6794	0.6694	−17.9512

The other best case is the combination of ENG-MNG which is unsatisfactory and oscillatory. If in the case of TM polarization, the desired band width is narrow, all the combinations may give good results for RCS reduction. Since for TM polarization, the electric field vector is parallel to the cylinder axis, the RCS reduction by lossless
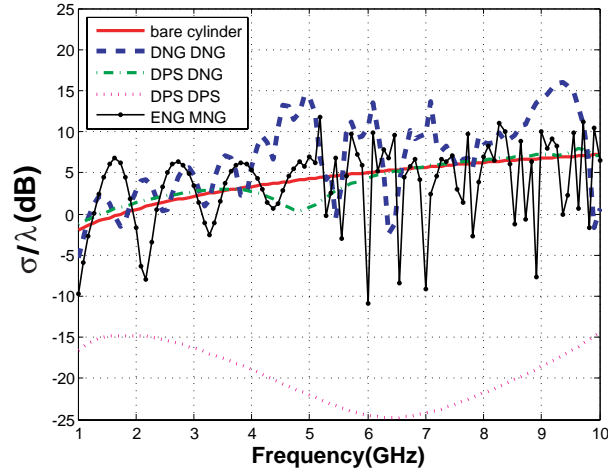
Figure 5. A comparison of the normalized RCS of a conducting cylinder ($a = 50$ mm) for TM polarization without coating and with two layer coating of nondispersive materials.

Table 6. Model parameters obtained after minimization of RCS of a conducting cylinder ($a = 50$ mm) in the frequency band [1–10] GHz for TE polarization with one layer coating made of dispersive DPS material.

Class of coating materials	Thickness layer of (mm)	Dispersion relation parameters after optimization
Relaxation-type	2.1868 mm	$\varepsilon_r = 1.2179$ $\mu_m = 23.5650$ $f_m = 1\,\text{GHz}$
Lossy Magnetic	0.1 mm	$\varepsilon_r = 1.0838$ $\mu_r = 24.9402$ $\mu_i = 1$ $\alpha = 1.2841 \times 10^{-6}$ $\beta = 1$
Lossy dielectric	0.2482 mm	$\varepsilon_r = 2.3703$ $\varepsilon_i = 1.3969$ $\alpha = 0.9880$ $\beta = 0.9728$ $\mu_r = 4.2816$

materials is more difficult than that for TE polarization.

Example 4. Consider a conducting cylinder of radius $a = 50$ mm covered with one layer of dispersive material under a normally incident TE plane wave. Three types of materials are separately considered, namely lossy dielectric, lossy magnetic and relaxation type. The optimized parameters are obtained for each case. The normalized optimum RCS for the bare and coated conducting cylinder are drawn versus frequency in Fig. 6. It is observed that considerable RCS reduction is achieved by the application of relaxation type material coating, whereas the lossy magnetic and electric materials do not lead to the reduction of RCS, although they may do so in a narrow bandwidth.
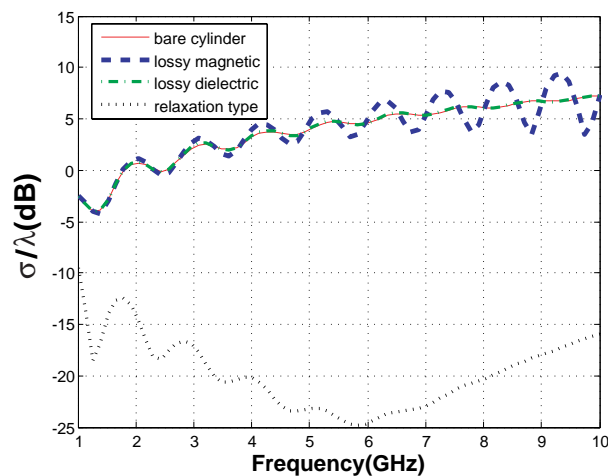

Figure 6. Minimized RCS of a conducting cylinder ($a = 50$ mm) for TE polarization without coating and with one layer of coating made of dispersive DPS (related to Table 6).

Example 5. Consider a conducting cylinder of radius $a = 50$ mm with one coating layer of dispersive metamaterial under normal incidence of a TE plane wave. The dispersive models for ε_r and μ_r are those of Drude and Lorentz, respectively. We consider three types of materials, namely rods only, rings only and rods & rings. The results of optimizations for each one of the metamaterials are summarized in Table 7. and the normalized optimum RCS curves versus frequency are drawn in Fig. 7. It is observed that the rods & rings coating is the best for RCS reduction.

Example 6. Consider a conducting cylinder of radius $a = 50$ mm with one layer of coating under normally incident TM polarized plane
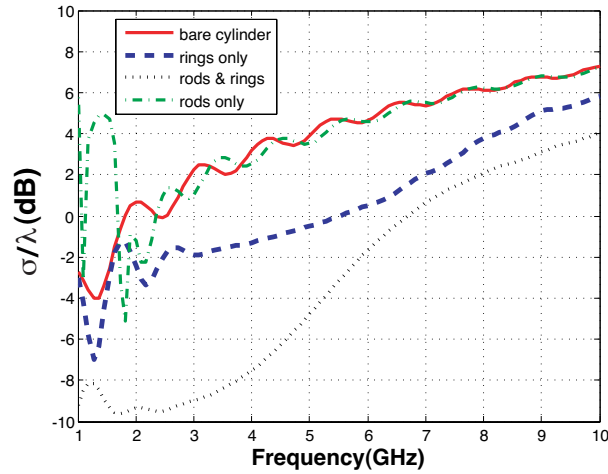
Figure 7. Minimized RCS of a conducting cylinder ($a = 50\,\text{mm}$) without coating and with one layer of coating made of dispersive metamaterial for TE polarization (related to Table 7).

Table 7. Model parameters obtained after minimization of RCS of a conducting cylinder ($a = 50\,\text{mm}$) with one layer coating made of dispersive metamaterial in the frequency band [1–10] GHz for TE polarization.

Class of coating materials	Thickness of layer (mm)	Dispersion relation parameters after optimization
Rods only	30 mm	$f_{ep} = 1.6767\,\text{GHz}$ $\gamma_e = 0.001\,\text{GHz}$
Ring only	29.7 mm	$f_{mo} = 4.7781\,\text{GHz}$ $f_{mp} = 4.4160\,\text{GHz}$ $\gamma_m = 5\,\text{GHz}$
Rods & Rings	30 mm	$f_{ep} = 2.9143\,\text{GHz}$ $\gamma_e = 5\,\text{GHz}$ $f_{mo} = 2.1960\,\text{GHz}$ $f_{mp} = 3.0465\,\text{GHz}$ $\gamma_m = 4.6490\,\text{GHz}$

wave. The coating materials that have provided the best reduction of RCS are relaxation type, rings only and rings & rods. The results for

the optimized RCS are given in Table 8 and drawn in Fig. 8. Again, the relaxation type material has provided the best reduction of RCS although rings & rods coating has caused a drastic reduction of RCS at $f = 7.8\,\text{GHz}$.
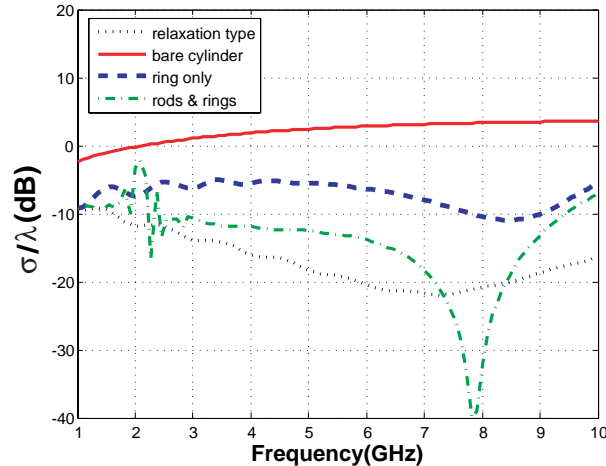

Figure 8. Minimized RCS of a conducting cylinder ($a = 50\,\text{mm}$) without coating and with one layer of coating made of different dispersive materials & metamaterials for TM polarization (related to Table 8).

In the following three examples, two layers are used for coating the conducting cylinder in order to achieve better reduction of RCS.

Example 7. Consider a conducting cylinder of radius $a = 50\,\text{mm}$ with two layers of coating made of common materials and metamaterials having dispersive characteristics under TE polarized plane wave normal incidence. Among various combinations of such materials for the two layers, only four cases are considered for the reduction of RCS. Due to the large number of variables, the optimization becomes quite time consuming. The resulting data are given in Table 9. The RCS versus frequency curves are drawn in Fig. 9.

It is observed that the case of both layers being made of rods & rings provides the least values of RCS.

Example 8. This example is the same as example 7, but with TM polarization. The results are given in Table 10 and Fig. 10. In this example as well as others, advantages of application of metamaterials for coating are noteworthy.

Example 9. This example is the same as Example 7, but with circular polarization. The results of RCS optimization for four cases

Table 8. Model parameters for minimized RCS of a conducting cylinder ($a = 50$ mm) with one layer of coating made of different dispersive materials & metamaterials in the frequency band [1–10] GHz for TM polarization.

Class of coating materials	Thickness of layer(mm)	Dispersion relation parameters after optimization
Relaxation-type	2.0790 mm	$\varepsilon_r = 1.4547$ $\mu_m = 24.5803$ $f_m = 1.0003$ GHz
Ring only	7.2119 mm	$f_{mo} = 2.3994$ GHz $f_{mp} = 8.9712$ GHz $\gamma_m = 5$ GHz
Rods & Rings	10.4942 mm	$f_{ep} = 9.071$ GHz $\gamma_e = 3.58$ GHz $f_{mo} = 2.6478$ GHz $f_{mp} = 10.2304$ GHz $\gamma_m = 4.7292$ GHz

of material coating are given in Table 11 and Fig. 11. It is seen that a combination of relaxation-type materials and metamaterials are the best for the reduction of RCS. Furthermore, this case has resulted in the least thickness for the two layers equal to 1 (cm).

Example 10. Reflection of EM wave in an arbitrary direction using metamaterial coating.

Suppose it is desired to maximize the EM reflection (or RCS) from a glass cylinder (with $\mu_r = 1$ and $\varepsilon_r = 5.25$ and radius $a = 35$ mm) in the direction $\varphi = \pm 30°$. The normally incident plane wave has TM polarization and is at frequency $f = 10$ GHz. A layer of material with variable thickness $(b - a)$, permittivity and permeability is placed on the cylinder. The RCS maximization algorithm based on MLS, GA and CG provided the following parameters for a DNG metamaterial and maximum reflection in the direction $\varphi = \pm 30°$.

$$b - a = 1.1369 \text{ mm}, \ \varepsilon_r = -1.9446, \ \mu_r = -0.4124.$$

The reflection pattern is shown in Fig. 12. It is seen that the main lobe is directed in the forward direction. The same design may be performed for a PEC cylinder.

Example 11. Invisible glass cylinder in the X-band with the application of metamaterials.

Table 9. Model parameters for minimization of RCS due to a conducting cylinder ($a = 50\,\text{mm}$) with two layers of coating made of dispersive materials & metamaterials in the frequency band [1–10] GHz for TE polarization.

| Class of coating materials	Thickness of layer (mm)	Dispersion relation parameters after optimization
First layer: Relaxation-type	11.7728	$\varepsilon_r = 12.5289$ $\mu_m = 3.1640$ $f_m = 1.0971\,\text{GHz}$
Second layer: Relaxation-type	1.6407	$\varepsilon_r = 1.7348$ $\mu_m = 13.7611$ $f_m = 2.0043\,\text{GHz}$
First layer: Relaxation-type	20.0912	$\varepsilon_r = 2.6932$ $\mu_m = 5.3423$ $f_m = 19.225\,\text{GHz}$
Second layer: Rods & Rings	3.5022	$f_{ep} = 7.7737\,\text{GHz}$ $\gamma_e = 4.7124\,\text{GHz}$ $f_{mo} = 2.5871\,\text{GHz}$ $f_{mp} = 4.7382\,\text{GHz}$ $\gamma_m = 3.8714\,\text{GHz}$
First layer: Rings only	2.2500	$f_{mo} = 10.2778\,\text{GHz}$ $f_{mp} = 6.9158\,\text{GHz}$ $\gamma_m = 4.8752\,\text{GHz}$
Second layer: Rods & Rings	11.5745	$f_{ep} = 7.6251\,\text{GHz}$ $\gamma_e = 3.5655\,\text{GHz}$ $f_{mo} = 1.1662\,\text{GHz}$ $f_{mp} = 8.6965\,\text{GHz}$ $\gamma_m = 4.9983\,\text{GHz}$
First layer: Rods & Rings	5.01696	$f_{ep} = 3.55967\,\text{GHz}$ $\gamma_e = 3.84294\,\text{GHz}$ $f_{mo} = 10.99295\,\text{GHz}$ $f_{mp} = 8.98339\,\text{GHz}$ $\gamma_m = 4.74019\,\text{GHz}$
Second layer: Rods & Rings	16.66038	$f_{ep} = 7.71387\,\text{GHz}$ $\gamma_e = 4.05248\,\text{GHz}$ $f_{mo} = 1.4311\,\text{GHz}$ $f_{mp} = 8.34629\,\text{GHz}$ $\gamma_m = 4.78006\,\text{GHz}$
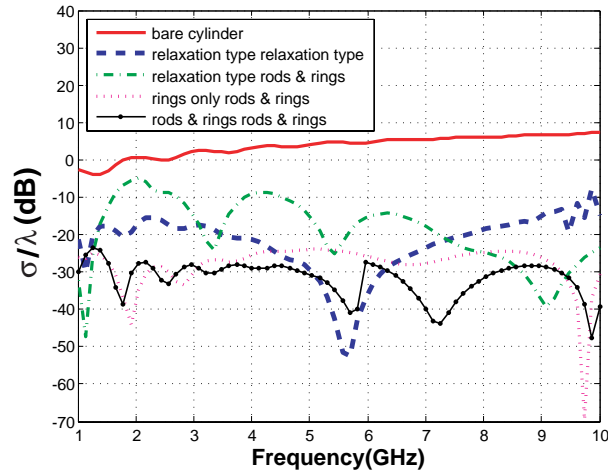
Figure 9. Minimized RCS of a conducting cylinder ($a = 50$ mm) without coating and with two layers of coating made of different dispersive common materials & metamaterials for TE polarization (related to Table 9).
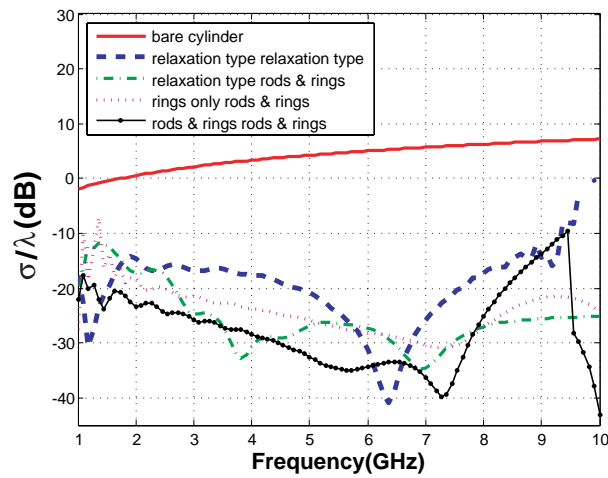

Figure 10. Normalized RCS of a conducting cylinder ($a = 50$ mm) without coating and with two layers of coating made of dispersive common materials & metamaterials for TM polarization (related to Table 10).

Table 10. Model parameters for minimization of RCS of a conducting cylinder ($a = 50\,\text{mm}$) with two layers of coating made of dispersive materials & metamaterials in the frequency band [1–10] GHz for TM polarization.

Class of coating materials	Thickness of layer (mm)	Dispersion relation parameters after optimization
First layer: Relaxation-type	23.3233	$\varepsilon_r = 4.7704$ $\mu_m = 8.3972$ $f_m = 2.1534\,\text{GHz}$
Second layer: Relaxation-type	3.5068	$\varepsilon_r = 1.5301$ $\mu_m = 2.5637$ $f_m = 9.7850\,\text{GHz}$
First layer: Relaxation-type	1.6244	$\varepsilon_r = 1.4048$ $\mu_m = 9.0673$ $f_m = 2.6907\,\text{GHz}$
Second layer: Rods & Rings	3.6470	$f_{ep} = 4.9220\,\text{GHz}$ $\gamma_e = 1.3825\,\text{GHz}$ $f_{mo} = 1.3346\,\text{GHz}$ $f_{mp} = 7.0657\,\text{GHz}$ $\gamma_m = 2.2118\,\text{GHz}$
First layer: Rings only	21.0698	$f_{mo} = 8.1461\,\text{GHz}$ $f_{mp} = 4.1679\,\text{GHz}$ $\gamma_m = 2.1244\,\text{GHz}$
Second layer: Rods & Rings	23.7085	$f_{ep} = 7.7162\,\text{GHz}$ $\gamma_e = 4.7101\,\text{GHz}$ $f_{mo} = 1.3765\,\text{GHz}$ $f_{mp} = 7.4827\,\text{GHz}$ $\gamma_m = 4.4042\,\text{GHz}$
First layer: Rods & Rings	24.60365	$f_{ep} = 8.94898\,\text{GHz}$ $\gamma_e = 2.89509\,\text{GHz}$ $f_{mo} = 21.01548\,\text{GHz}$ $f_{mp} = 10.67497\,\text{GHz}$ $\gamma_m = 4.31605\,\text{GHz}$
Second layer: Rods & Rings	29.2829	$f_{ep} = 7.37042\,\text{GHz}$ $\gamma_e = 4.81552\,\text{GHz}$ $f_{mo} = 1.02431\,\text{GHz}$ $f_{mp} = 7.0456\,\text{GHz}$ $\gamma_m = 4.44306\,\text{GHz}$

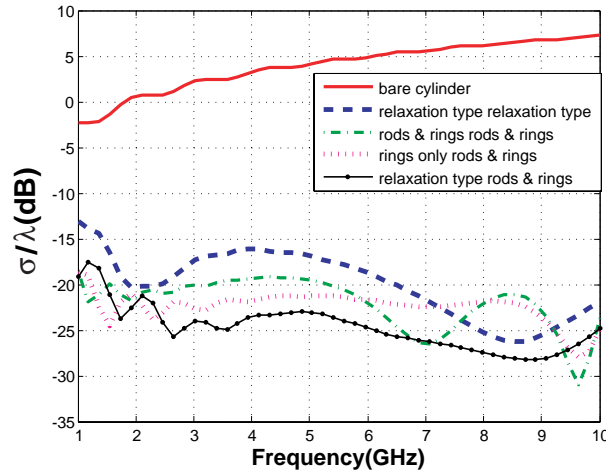**Figure 11.** Normalized RCS of a conducting cylinder ($a = 50\,\text{mm}$) without coating and with two layers of coating made of dispersive materials & metamaterials for circular polarization (related to Table 11).
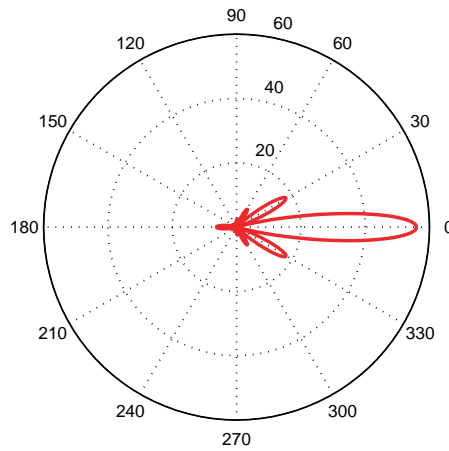

Figure 12. Polar plot of RCS for a glass cylinder with a layer of DNG metamaterial.

Consider a glass cylinder of radius $a = 15\,\text{mm}$ and parameters $\varepsilon_r = 4$, $\mu_r = 1$ under a normally incident plane wave with TM polarization in the X-band (8–12 GHz). It is desired to minimize the back scattered RCS by using a coating layer of lossy and dispersive

Table 11. Model parameters for minimization of RCS due to a conducting cylinder ($a = 50\,\text{mm}$) with two layers of coating made of dispersive materials & metamaterials in the frequency band [1–10] GHz for circular polarization.

| Class of coating materials	Thickness of layer (mm)	Dispersion relation parameters after optimization
First layer: Relaxation-type	11.43071	$\varepsilon_r = 4.27893$ $\mu_m = 5.59839$ $f_m = 1.00207\,\text{GHz}$
Second layer: Relaxation-type	1.35436	$\varepsilon_r = 1.62729$ $\mu_m = 7.2224$ $f_m = 5.14879\,\text{GHz}$
First layer: Rods & Rings	19.33092	$f_{ep} = 14.57004\,\text{GHz}$ $\gamma_e = 1.16466\,\text{GHz}$ $f_{mo} = 13.48752\,\text{GHz}$ $f_{mp} = 4.22294\,\text{GHz}$ $\gamma_m = 4.02466\,\text{GHz}$
Second layer: Rods & Rings	13.40032	$f_{ep} = 6.62216\,\text{GHz}$ $\gamma_e = 3.82287\,\text{GHz}$ $f_{mo} = 1.10228\,\text{GHz}$ $f_{mp} = 7.56018\,\text{GHz}$ $\gamma_m = 4.92624\,\text{GHz}$
First layer: Rings only	3.39905	$f_{mo} = 10.67061\,\text{GHz}$ $f_{mp} = 7.48301\,\text{GHz}$ $\gamma_m = 4.97807\,\text{GHz}$
Second layer: Rods & Rings	13.47335	$f_{ep} = 7.21621\,\text{GHz}$ $\gamma_e = 4.25091\,\text{GHz}$ $f_{mo} = 1.00628\,\text{GHz}$ $f_{mp} = 7.84661\,\text{GHz}$ $\gamma_e = 4.98687\,\text{GHz}$
First layer: Relaxation-type	3.62882	$\varepsilon_r = 1.54758$ $\mu_m = 2.63786$ $f_m = 3.79167\,\text{GHz}$
Second layer: Rods & Rings	5.88448	$f_{ep} = 3.61918\,\text{GHz}$ $\gamma_e = 3.43578\,\text{GHz}$ $f_{mo} = 1.00105\,\text{GHz}$ $f_{mp} = 5.90441\,\text{GHz}$ $\gamma_m = 3.3183\,\text{GHz}$
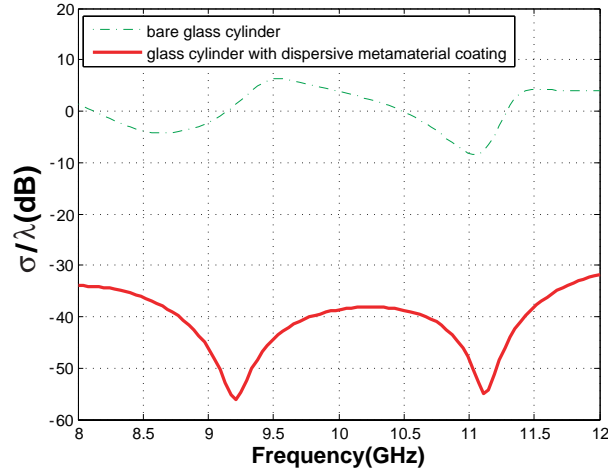
Figure 13. Backscattered RCS of a bare glass cylinder and that of a cylinder with a MTM coating.

metamaterials.

The minimization of RCS is performed by the combination of MLS, GA and CG on the variables of the layer thickness and parameters of dispersion models. The RCS of a bare glass cylinder and that of the cylinder covered by metamaterial are drawn in Fig. 13 for comparison. The optimized parameters are:

$$b - a = 7.49 \, \text{mm}, \ \ f_{ep} = 26.0214 \, \text{GHz}, \ \ \gamma_e = 4.2989 \, \text{GHz}$$

$$f_{mo} = 1.0012 \, \text{GHz}, \ \ f_{mp} = 25.2375 \, \text{GHz}, \ \ \gamma_m = 3.0042 \, \text{GHz}$$

The reduction of RCS by 40 dB across the X-band is achieved. The behavior of all the types of materials namely DPS, DNG, ENG and MNG are observed in the X-band, which call for careful attention to the sign of various parameters.

7. CONCLUSIONS

In this paper the addition theorem for cylindrical waves is extended for the analysis of multilayered cylindrical structures for minimization or maximization of RCS, under normally incident plane waves of arbitrary polarizations. A combination of common materials and metamaterials with various dispersion models are used for the coating layers of cylindrical core. A novel combination of MLS, GA and CG is used to speed up the convergence of the algorithm to the

global minimum (or maximum) point and to avoid trapping in local minima. It is observed that the reduction of RCS in a wide frequency bandwidth is not achievable by using merely common materials. However, application of various metamaterials for coatings of cylindrical structures effectively reduces RCS in a wide band. Optimum design of wideband RCS depends on the incident TE or TM plane wave polarizations, which indicate that the best design should be based on circular polarization. Various examples of RCS reduction for PEC or dielectric cylindrical cores are provided and appropriate conclusions are derived. Furthermore, the procedure for selecting the correct sign of the real and imaginary parts of the lossy and lossless metamaterial parameters (as computed by their appropriate formulas) are described in detail.

REFERENCES

1. Knot, E. F., J. F. Shaeffer, and M. T. Tuley, *Radar Cross-Section*, Artech House, Norwood, MA, 1986.

2. Skolnik, M. I., *Radar Handbook*, McGrawhill, NY, 1986.

3. Ishimaru, A., *Electromagnetic Wave Propagation, Radiation, and Scattering*, Prentice Hall, Englewood Cliffs, 1991.

4. Vinoy, K. J. and R. M. Jha, *Radar Absorbing Materials: From Theory to Design and Characterization*, Kluwer Academic Publishers, Masachusetts, 1996.

5. Ramprecht, J. and D. Sjeberg, "Biased magnetic materials in RAM applications," *Progress In Electromagnetics Research*, PIER 75, 85–117, 2007.

6. Chamaani, S., S. A. Mirta, M. Teshnehlab, M. A. Shooredeli, and V. Seydi, "Modified multi-objective particle swarm optimization for electromagnetic absorber design," *Progress In Electromagnetics Research*, PIER 79, 353–366, 2008.

7. Pendry, J. B., A. J. Holden, W. J. Stewart, and I. Youngs, "Extremely low frequency plasmons in metallic mesostructure," *Phys. Rev. Lett.*, Vol. 76, No. 25, 4773–4776, 1996.

8. Pendry, J., A. Holden, and W. Stewart, "Magnetism from conductors and enhanced nonlinear phenomena," *IEEE Trans. Microwave Theory Tech.*, Vol. 47, No. 18, 2075–2084, 1999.

9. Oraizi, H. and A. Abdolali, "Ultra wide band RCS optimization of multilayerd cylindrical structures for arbitrarily polarized incident plane waves," *Progress In Electromagnetics Research*, PIER 78, 129–157, 2008.

10. Lee, Y. S., C. C. Chiu, and Y. S. Lin, "Electromagnetic imaging for an imperfectly conducting cylinder buried in a three-layer structure by the genetic algorithm," *Progress In Electromagnetics Research*, PIER 48, 27–44, 2004.

11. Yang, J., L. W. Li, K. Yasumoto, and C. H. Liang, "Two-dimensional scattering of a Gaussian beam by a periodic array of circular cylinders," *IEEE Transactions on Geoscience and Remote Sensing*, Vol. 43, No. 2, 280–285, 2005.

12. Wang, X. D., Y. B. Gan, and L. W. Li, "Electromagnetic scattering by partially buried PEC cylinder at the dielectric rough surface interface: TM case," *IEEE Antennas and Wireless Propagation Letters*, Vol. 2, 319–322, 2003.

13. Zhang, M., T. S. Yeo, L. W. Li, and M. S. Leong, "Electromagnetic scattering by a multilayer gyrotropic bianisotropic circular cylinder," *Progress In Electromagnetics Research*, PIER 40, 91–111, 2002.

14. Yang, J., L. W. Li, and C. H. Liang, "Two-dimensional scattering by a periodic array of gyrotropic cylinders embedded in a dielectric slab," *IEEE Antennas and Wireless Propagation Letters*, Vol. 2, No. 1, 18–21, 2003.

15. Veselago, V., "The electrodynamics of substances with simultaneously negative values of ε and μ," *Soviet Physics Uspekhi*, Vol. 10, No. 4, 509–514, 1968.

16. Xu, Z., W. Lin, and L. Kong, "Controllable absorbing structure of metamaterial at microwave," *Progress In Electromagnetics Research*, PIER 69, 117–125, 2007.

17. Liu, S.-H., C.-H. Liang, W. Ding, L. Chen, and W.-T. Pan, "Electromagnetic wave propagation through a slab waveguide of uniaxially anisotropic dispersive metamaterial," *Progress In Electromagnetics Research*, PIER 76, 467–475, 2007.

18. Moss, C. D., T. M. Grzegorczyk, Y. Zhang, and J. A. Kong, "Numerical studies of left handed metamaterials," *Progress In Electromagnetics Research*, PIER 35, 315–334, 2002.

19. Oraizi, H., "Application of the method of least squares to electromagnetic engineering problems," *IEEE Antenna and Propagation Magazine*, Vol. 48, No. 1, 50–75, 2006.

20. Michielssen, E., J.-M. Sajer, S. Ranjithan, and R. Mittra, "Design of lightweight, broad-band microwave absorbers using genetic algorithms," *IEEE Trans. Microwave Theory Tech.*, Vol. 41, No. 67, 1024–1031, June/July 1993.

21. Xu, Z., H. Li, Q.-Z. Liu, and J.-Y. Li, "Pattern synthesis of conformal antenna array by the hybrid genetic algorithm," *Progress In Electromagnetics Research*, PIER 79, 75–90, 2008.

22. Meng, Z., "Autonomous genetic algorithm for functional optimization," *Progress In Electromagnetics Research*, PIER 72, 253–268, 2007.

23. Qing, A. and C. K. Lee, "Microwave imaging of parallel perfectly conducting cylinders using real-coded genetic algorithm coupled with Newton-Kantorivitch method," *Progress In Electromagnetics Research*, PIER 28, 275–294, 2000.

24. Choi, S., "Application of conjugate gradient method for optimum array processing," *Progress In Electromagnetics Research*, PIER 05, 589–624, 1991.

25. Tang, C. C. H., "Backscattering from dielectrically coated infinite cylindrical obstacles," Ph.D. Thesis, Harvard University, 1956.